AIP | Applied Physics Letters

Design concepts of terahertz quantum cascade lasers: Proposal for terahertz laser efficiency improvements

Tillmann Kubis, Saumitra Raj Mehrotra, and Gerhard Klimeck

Citation: Appl. Phys. Lett. **97**, 261106 (2010); doi: 10.1063/1.3524197
View online: http://dx.doi.org/10.1063/1.3524197
View Table of Contents: http://apl.aip.org/resource/1/APPLAB/v97/i26
Published by the American Institute of Physics.

Design concepts of terahertz quantum cascade lasers: Proposal for terahertz laser efficiency improvements

Tillmann Kubis,[a] Saumitra Raj Mehrotra, and Gerhard Klimeck
Network for Computational Nanotechnology, Birk Nanotechnology Center, School of Electrical and Computer Engineering, Purdue University, West Lafayette, Indiana 47907, USA

(Received 24 September 2010; accepted 11 November 2010; published online 28 December 2010)

Conceptual disadvantages of typical resonant phonon terahertz quantum cascade lasers (THz-QCLs) are analyzed. Alternative designs and their combination within a concrete device proposal are discussed to improve the QCL performance. The improvements are (1) indirect pumping of the upper laser level, (2) diagonal optical transitions, (3) complete electron thermalization, and (4) materials with low effective electron masses. The nonequilibrium Green's function method is applied to predict stationary electron transport and optical gain. The proposed THz-QCL shows a higher optical gain, a lower threshold current, and a higher operation temperature. Alloy disorder scattering can worsen the QCL performance.
 [doi:10.1063/1.3524197]

A wide range of scientific and commercial applications requires high power and coherent terahertz sources since the characteristic excitation lines of many molecules lie within the terahertz spectral region.[1–3] Terahertz quantum cascade lasers (THz-QCLs) are promising candidates to supply intense coherent terahertz light. Since the realization of THz-QCLs by Koehler *et al.*,[4] the performance of these lasers has been significantly improved, but their operation is still limited to cryogenic temperatures.

To increase the maximum operating temperature and to increase the output power, several disadvantages of the commonly used resonant phonon THz-QCL design are analyzed. Subsequently, alternative design concepts and their combination within an efficient THz-QCL are presented. Finally, the calculated data of a concrete example of the proposed design concept are presented. Although the various parameters of this proposed QCL have not been optimized, this example shows a much higher optical gain and a higher operating temperature.

The mechanisms that are responsible for optical gain in a typical resonant phonon THz-QCL can be deduced from Fig. 1(a). It depicts a schematic of the conduction band profile and the resonant states at an applied electric field close to threshold. The upper laser level (labeled 4) is aligned with the injector state 5 in the leftmost source-sided quantum well and therefore gets filled by resonant tunneling. The spatial overlap of the lower laser level 3 with the upper one is very large to guarantee a large oscillator strength of the optical transition. The lower laser level 3 gets efficiently emptied by two mechanisms. State 3 is aligned with state 2 of the rightmost well, which allows its coherent depletion by tunneling. Second, the energy difference between this state and the lowest resonant state (1) matches the energy of an LO-phonon, which leads to an additional depletion by the resonant emission of LO-phonons. The alignment of the resonant states as well as the electric field at threshold are chosen such that the potential drop per period ($e\Phi_{th}$) equals the sum of the energy of one emitted photon (E_γ) and the energy of one LO-phonon (E_{LO}).

There are several issues with this design concept that intrinsically lower the overall device performance:

Coherent filling. The alignment of the injector state 5 with the upper laser level 4 allows for a delocalization of the upper laser level beyond the area of the lower laser level 3. This reduces the oscillator strength as well as the lifetime of electrons in the upper laser level. In addition, multibarrier tunneling across a complete QCL period becomes more likely if the upper laser level is not confined well enough.[5]

Direct laser transition. The large spatial overlap of the upper (4) and lower (3) laser level significantly increases the probability of nonluminescent transitions. Accordingly, it has been shown in previous work that the optical gain of this kind of THz-QCL is dramatically reduced by the electron scattering on rough interfaces.[6] Scattering on rough interfaces suggests to increase the laser frequency: a larger energy separation between the laser levels increases the scattered in-plane momentum and thereby reduces the scattering probability.[7,8] However, the thermally activated LO-phonon emission of electrons in the upper laser level is another important degradation mechanism.[9] The LO-phonon emission suggests a smaller laser frequency: the larger the energy difference between the laser levels 3 and 4 is, the more electrons meet the minimum energy requirement for the phonon emission and the smaller is the scattered in-plane momentum. The conflict of both effects limits the improvement options in typical THz-QCLs.

Incomplete thermalization. Typical THz-QCLs are designed such that the potential drop per period at threshold bias equals the sum of the emitted photon energy and the energy of one LO-phonon. On the average, however, most electrons pass THz-QCL periods without emitting light.[6] It has been shown in previous work that electrons that pass a period without emitting a photon get heated up with respect to their in-plane distribution.[6] When these electrons are thermalized in subsequent periods, the population inversion is significantly reduced. The resulting overall optical gain can be lowered by almost a factor of 2.[6]

[a]Electronic mail: tkubis@purdue.edu.

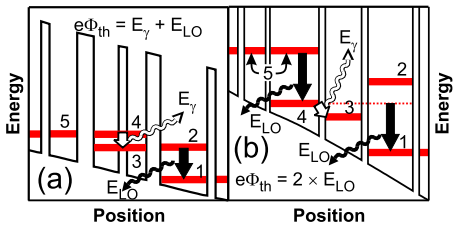

FIG. 1. (Color online) Schematics of the conduction band (black) and the resonant states (thick) of a typical resonant phonon THz-QCL (a) and the presently proposed design concept (b) at threshold voltage Φ_{th}. Arrows depict emitted photons (white) and phonons (black). The potential drop $e\Phi_{th}$ in the typical design (a) equals the energy of one photon and one phonon. In the proposed design (b), it is equal to the energy of two phonons.

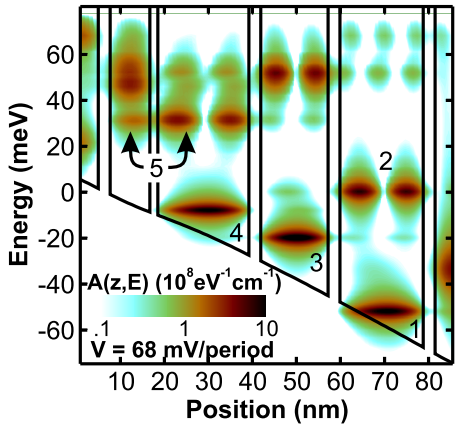

FIG. 2. (Color online) Calculated conduction band profile (line) and contour plot of the energy and spatially resolved spectral function $A(z,E)$ at vanishing in-plane momentum in the proposed QCL at the threshold bias voltage of 68 mV per period and a lattice temperature of 100 K. The zero in energy marks the chemical potential of the source.

Material properties. It is very common to use unstrained $Al_{0.15}Ga_{0.85}As/GaAs$ quantum well heterostructures for resonant phonon THz-QCLs. Meanwhile, it is known that the optical gain is proportional to $(1/m^*)^{3/2}$, with the effective electron mass m^*.[10] Therefore, designing the THz-QCLs based on materials with lower effective electron masses can lead to a higher optical gain.

These issues are solved in a THz-QCL design proposed in the next paragraphs. The mechanisms that lead to occupation inversion and optical gain in this design are depicted in Fig. 1(b) with a schematic of the conduction band profile and the resonant states at an applied electric field close to threshold. The upper laser level 4 is filled by electrons of the injector state 5 that resonantly emit an LO-phonon. The lower laser level 3 is spatially separated from the upper laser level forcing the optical transition to be diagonal. The lowest level of the collector well (1) is exactly one LO-phonon energy below the upper laser level (4). This guarantees that most of the electrons (i.e., the nonluminescent ones) are thermalized in each QCL period. Compared to the conventional resonant phonon design of Fig. 1(a), this concept has several advantages:

Indirect pumping. The upper laser level is well confined within a single quantum well. This reduces the chance of coherent leakage to the next QCL stage. In addition, the number of (rough) interfaces that can influence the upper state lifetime is reduced. As has been shown in previous work, just indirect pumping alone can increase the peak gain by a factor of approximately 3.[9] Recent experimental and theoretical works confirm that indirect pumping can improve the device performance.[11,12]

Diagonal transitions. Nonluminescent transitions between the laser levels are suppressed because the spatial overlap is much smaller than in the typical design. Please note that the optical transition is proportional to the transition dipole element, which has a different spatial characteristic than nonluminescent transitions. Previous work has demonstrated that the optical gain of a diagonal transition is much less sensitive to scattering on rough interfaces than direct transitions.[13] It is worth to note that the THz-QCL with a temperature limit of 186 K utilizes diagonal optical transitions.[14] Once the nonluminescent elastic transitions are suppressed, the energy difference between the laser levels can be reduced in order to suppress the probability for thermally activated LO-phonon emission of electrons in the upper laser level.

Complete thermalization. The energy balance of the QCL in Fig. 1(b) is neglecting the photon energy. In this way, it is guaranteed that the majority of electrons, i.e., those that are not emitting light, are thermalized within each period. Therefore, nonperiodic effects, which have shown to significantly worsen the QCL performance, are efficiently suppressed.[6,15]

Low effective mass. The combination of $In_{0.53}Ga_{0.47}As$ and $GaAs_{0.51}Sb_{0.49}$ layers instead of the commonly used $Al_{0.15}Ga_{0.85}As/GaAs$ material system has the advantage of lower effective electron masses. This material system has recently been shown to yield optical intersubband transitions.[16]

All these suggestions have been combined into a concrete $In_{0.53}Ga_{0.47}As/GaAs_{0.51}Sb_{0.49}$ QCL device design. Starting from the leftmost barrier in Fig. 1(b), one period of the indirect-pumped QCL sequence was taken as **2.7**/9/**1.8**/20.7/**2.7**/15.3/**2.7**/18.9 nm. The bold and regular numbers represent $GaAs_{0.51}Sb_{0.49}$ and $In_{0.53}Ga_{0.47}As$ layers, respectively. The underlined 9-nm-thick quantum well is the only n-doped region at the level of 2.04×10^{16} cm^{-3}. We have applied the nonequilibrium Green's function (NEGF) method on the stationary charge transport and the linear optical response of this QCL. Thereby, the QCL is considered as an open quantum device with multiquantum well leads. Electrons within each lead are distributed according to Fermi distributions. Therefore, all electrons enter the QCL device in equilibrium distributions and nonequilibrium electrons that leave the device are thermalized within the leads. Incoherent scattering of electrons on optical and acoustic phonons, charged impurities, rough interfaces, and random alloy disorder is included. The electron-electron interaction in the Hartree approximation is taken into account. Please refer to Ref. 6 for implementation details. Figure 2 shows the spectral function $A(z,E)$ at zero in-plane momentum of the proposed QCL resulting from this NEGF calculation. Resonant states correspond with peaks of $A(z,E)$. We have assumed an LO-phonon energy of 34 meV in the composed material system and designed the potential drop at threshold bias commensurable with this LO-phonon energy. The alloy scattering potential δV^{TB} is estimated from empirical tight-binding parameters to be 0.493 eV for $In_{0.53}Ga_{0.47}As$ and 0.36 eV for $GaAs_{0.51}Sb_{0.49}$.[17–19] All remaining material parameters are taken from Ref. 10. The calculated emission energy of the present laser is 10 meV. Figure 3 compares the calculated peak gain as a function of the lattice temperature

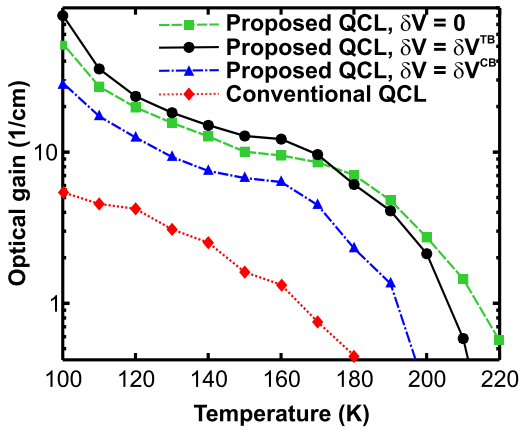

FIG. 3. (Color online) Calculated peak optical gain as a function of the lattice temperature. The conventional resonant phonon QCL of Ref. 20 (diamonds) exhibits a smaller optical gain than the presently proposed design (spheres) for all temperatures when the alloy scattering potentials δV^{TB} are estimated from tight binding calculations δV^{TB}. The triangles show the results of the proposed QCL with the approximate alloy scattering potentials δV^{CB} due to conduction band differences of the binary alloys. The squares depict the proposed gain without alloy scattering. Lines are meant to guide the eye.

in the present QCL to the conventional THz-QCL of Ref. 20 with the same effective doping density per period. The proposed design yields a higher optical gain for all temperatures and has an about 20 K higher maximum operation device temperature. Note that the high threshold current of the conventional design heats the QCL by 20–50 K above the heat sink temperature.[21,22] It is also worth to mention that the threshold current density of the proposed design at 40 K lattice temperature is 0.13 kA/cm^2. This is approximately four times smaller than in the conventional design of the same effective doping and temperature.[20] Rough interfaces reduce the optical gain of the proposed design by only about 40% (instead of 90% in the old design) and tend to stabilize the carrier transport. In particular, the calculations predict a higher current density if the QCL is grown with the source-sided barrier interfaces being rough and the opposite interfaces being smooth. The implemented alloy scattering potential in $In_{0.53}Ga_{0.47}As$ agrees with experimental findings.[23] However, some authors use the conduction band difference of the binary alloys δV^{CB} instead (about 1 eV for $In_{0.53}Ga_{0.47}As$ and 0.1 eV for $GaAs_{0.51}Sb_{0.49}$). Figure 3 shows the influence of the alloy disorder scattering on the proposed QCL. At low temperatures, the filling of the upper laser level and the optical gain is slightly improved by alloy disorder scattering. Once this level filling gets saturated by high disorder potentials δV or at high temperatures by enhanced phonon scattering (at about 175 K in Fig. 3), alloy disorder scattering preferably supports nonradiative losses and reduces the optical gain.

In conclusion, several conceptual disadvantages of common resonant phonon THz-QCLs have been discussed. Alternative concepts have been presented that avoid all of these disadvantages and result in THz-QCLs with improved laser performance. A concrete THz-QCL that combines all alternative design concepts has been proposed. Nonequilibrium Green's function calculations of this proposed QCL show significantly higher optical gain, a higher maximum temperature, and an approximately four times lower threshold current density than in a comparable conventional THz-QCL. It is shown that a strong alloy disorder scattering can worsen the optical output performance.

This work has been supported by the Austrian Scientific Fund FWF (Grant No. SFB-IRON) and the National Science Foundation (NSF) (Grant Nos. OCI-0749140, EEC-0228390, and ECCS-0701612). Computational resources of nanoHUB.org are gratefully acknowledged.

[1] J. R. Gao, J. N. Hovenier, Z. Q. Yang, J. J. A. Baselmans, A. Baryshev, M. Hajenius, T. M. Klapwijk, A. J. L. Adam, T. O. Klaassen, B. S. Williams, S. Kumar, Q. Hu, and J. L. Reno, Appl. Phys. Lett. **86**, 244104 (2005).
[2] H.-W. Hübers, S. G. Pavlov, H. Richter, A. D. Semenov, L. Mahler, A. Tredicucci, H. E. Beere, and D. A. Ritchie, Appl. Phys. Lett. **89**, 061115 (2006).
[3] A. W. M. Lee, Q. Qin, S. Kumar, B. S. Williams, Q. Hu, and J. L. Reno, Appl. Phys. Lett. **89**, 141125 (2006).
[4] R. Köhler, A. Tredicucci, F. Beltram, H. E. Beere, E. H. Linfield, A. G. Davies, D. A. Ritchie, R. C. Iotti, and F. Rossi, Nature (London) **417**, 156 (2002).
[5] T. Kubis and P. Vogl, Laser Phys. **19**, 762 (2009).
[6] T. Kubis, C. Yeh, P. Vogl, A. Benz, G. Fasching, and C. Deutsch, Phys. Rev. B **79**, 195323 (2009).
[7] R. Lake, G. Klimeck, R. C. Bowen, and D. Jovanovic, J. Appl. Phys. **81**, 7845 (1997).
[8] B. K. Ridley, *Quantum Processes in Semiconductors* (Oxford, New York, 1982).
[9] H. Yasuda, T. Kubis, P. Vogl, N. Sekine, I. Hosako, and K. Hirakawa, Appl. Phys. Lett. **94**, 151109 (2009).
[10] E. Benveniste, A. Vasanelli, A. Delteil, J. Devenson, R. Teissier, A. Baranov, A. M. Andrews, G. Strasser, I. Sagnes, and C. Sirtori, Appl. Phys. Lett. **93**, 131108 (2008).
[11] A. Wacker, Appl. Phys. Lett. **97**, 081105 (2010).
[12] S. Kumar, C. W. I. Chan, Q. Hu, and J. L. Reno, *Conference on Lasers and Electro-Optics (CLEO) and the Quantum Electronics and Laser Science Conference (QELS)* (Optical Society of America, Washington, D.C., 2010), Paper No. CThU1.
[13] T. Kubis, *Quantum Transport in Semiconductor Nanodevices*, edited by G. Abstreiter, M. C. Amann, M. Stutzmann, and P. Vogl (Verein zur Förderung des Walter Schottky Instituts der Technischen Universität München e.V., Garching, 2009), http://nanohub.org/resources/8612.
[14] S. Kumar, Q. Hu, and J. L. Reno, Appl. Phys. Lett. **94**, 131105 (2009).
[15] T. Kubis and P. Vogl, J. Phys.: Conf. Ser. **193**, 012063 (2009).
[16] M. Nobile, H. Detz, E. Mujagić, A. M. Andrews, P. Klang, W. Schrenk, and G. Strasser, Appl. Phys. Lett. **95**, 041102 (2009).
[17] T. B. Boykin, G. Klimeck, R. C. Bowen, and F. Oyafuso, Phys. Rev. B **66**, 125207 (2002).
[18] G. Hegde and G. Klimeck, unpublished parameters; G. Klimeck, R. C. Bowen, T. B. Boykin, C. Salazar-Lazaro, T. A. Cwik, and A. Stoica, Superlattices Microstruct. **27**, 77 (2000).
[19] S. Krishnamurthy, A. Sher, and A.-B. Chen, Appl. Phys. Lett. **47**, 160 (1985).
[20] A. M. Andrews, A. Benz, C. Deutsch, G. Fasching, K. Unterrainer, P. Klang, W. Schrenk, and G. Strasser, Mater. Sci. Eng., B **147**, 152 (2008).
[21] H. Callebaut, S. Kumar, B. S. Williams, Q. Hu, and J. L. Reno, Appl. Phys. Lett. **83**, 207 (2003).
[22] M. S. Vitiello, G. Scarmacio, V. Spagnolo, B. S. Williams, S. Kumar, and Q. Hu, Appl. Phys. Lett. **86**, 111115 (2005).
[23] P. K. Basu and B. R. Nag, Appl. Phys. Lett. **43**, 689 (1983).